Nano Energy (2012) 1, 25–41

Available online at www.sciencedirect.com

SciVerse ScienceDirect

journal homepage: www.elsevier.com/locate/nanoenergy

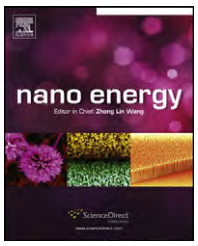

REVIEW

Plasmonic nano-lasers

Yin Yin[a], Teng Qiu[a,b,*], Jiaqi Li[a], Paul K. Chu[b,**]

[a]*Department of Physics, Southeast University, Nanjing 211189, PR China*
[b]*Department of Physics and Materials Science, City University of Hong Kong, Tat Chee Avenue, Kowloon, Hong Kong, PR China*
Available online 17 October 2011

KEYWORDS
Plasmonics;
Nano-laser;
Nano-energy;
Resonant cavity;
Dark mode

Abstract
Development of a coherent, intense, ultrafast source of optical energy focused to a nano-scale area enables the integration of thousands of them on a single chip to power an optical computer. Very intense, ultrafast, temporarily coherent pulses of nano-localized optical fields are thus of fundamental interest and have many applications in integrated nano-photonics. This paper reviews the mechanism associated with plasmonic nano-lasers and general guidelines pertaining to device design. Recent results show that a plasmonic nano-laser effectively overcomes many of the difficulties and limitations of plasmonics and has enormous potential in sub-wavelength photonic circuits and fundamental investigation of single-molecular events. Future challenges and research directions are also discussed.

Introduction

Lasers first experimentally demonstrated by Schawlow and Townes [1] are among the most important inventions in the 20th century. The ability to generate intense and coherent optical energy has spurred ground breaking research activities in micro- and nano-scale materials in the past decades. Deeper exploration of the micro- and nano-world requires extremely small, ultrafast, and coherent laser sources to concentrate optical energy into regions with sub-wavelength dimensions. However, advances have been hampered by conventional light sources because their size is constrained by the diffraction limit. Although some devices offer near-field optical energy [2–5] by adopting exit apertures with nano-dimensions, photon transport in the nanostructures is still not well understood. A nano-laser possessing a tiny cavity has a much smaller physical scale than a traditional laser and photonic crystals [6] have been developed to address the diffraction limitation. However, since conventional lasers are based on optical pumping and stimulated emission, it is difficult to produce a nano-scale cavity and overcome the diffraction limitation so that a beam of light with size smaller than its wavelength can be generated.

A plasmonic nano-laser is different from a conventional laser in that surface plasmons (SPs) instead of photons are used to amplify the radiation by stimulated emission [7]. SPs, a near-field phenomenon of surface electron oscillations, originate from the interactions between incident electromagnetic (EM) field and free electrons in metals such as silver and gold. The resonant excitations on the micro- or nano-scale metal structures tend to form highly localized SP with large EM field enhancement effects and good spatial confinement on the sub-wavelength scale, thus avoiding the limitation imposed by diffraction. In particular, the

*Corresponding author. Tel.: +86 25 52090600 8210; fax: +86 25 52090600 8204.
**Corresponding author. Tel.: +852 34427724; fax: +852 34420542.
E-mail addresses: tqiu@seu.edu.cn (T. Qiu), paul.chu@cityu.edu.hk (P.K. Chu).

2211-2855/$ - see front matter © 2011 Elsevier Ltd. All rights reserved.
doi:10.1016/j.nanoen.2011.09.002

nano-scale interface between a dielectric and metal supports some special EM modes such as SP polariton (SPP). SPP propagating along the interface is a transverse magnetic polarized optical surface wave bounded by the metal-dielectric border via coupling between the EM and longitudinal surface charge density oscillations in the metal [8]. When light irradiates the metal-dielectric interface, oscillations of free electrons in the metal are hindered by the dielectric border, which prevents the electrons from entering and forces them to move in waves along the nano-scale metal-dielectric interface. Meanwhile, a metal nanostructure with a large light absorption cross section is capable of confining the resonant energy into the localized nano-area by collective electron oscillations. The highly localized optical fields from SPs are confined into tiny spots with nano- or sub-wavelength dimensions. While traditional lasers suffer from diffraction effects in this size regime, the strong localized enhancement and sub-wavelength confinement lead to spatial localization in dimensions well below the diffraction limit thus making nano-scale integrated photonic circuits possible [9-12]. For example, Stockman has theoretically predicted SPPs propagation in a tapered plasmonic waveguide [13]. Rapid adiabatic nano-focusing of energy in three dimensions takes place on the tip and the local field and energy density are increased by three folds and orders of magnitude, respectively. In a plasmonic nano-laser, electron oscillations are coupled directly with the localized optical modes and the coupling can be modulated by the dielectric environment as well as size and shape of the metal nanostructures. Consequently, the low coupling efficiency and unavailability of individual optical modes can be circumvented.

The gain medium, which is an essential part of a traditional laser serving as the pumping and resonance cavity, plays a likewise important role in a nano-laser in order to maintain the population inversion in the multilevel system. The resonant cavity which serves to stimulate more light emission with the same phase by reflecting the light back and forth in a traditional laser is substituted by metal nanostructures such as nano-shells [14,15] in order to generate the initial SPs around the nano-scale metal-dielectric interface. The concept of SP amplification by stimulated emission of radiation (spaser) has recently been introduced [7] and demonstrated experimentally [16]. The energy transfer from the gain medium to SPs spurs SP resonance mostly with the same mode and more plasmonic modes are available for lasing radiation. Fig. 1 illustrates the important principles of lasing by stimulated emission amplification [17]. Electron-hole pairs in the semiconductor quantum dots (QDs) are generated by external pumping and population inversion. The QDs relax non-radiatively to an excitonic or multi-excitonic state caused by carrier multiplication, and the excitation energy is transformed to resonant SPs on the metal nanostructures instead of conversion to photons by exciton recombination. However, not all the SP excitations in the localized nano-field are necessarily coupled to the photonic modes simultaneously to emit light at a certain wavelength because of stimulated emission of SPs in the dark modes coupled to the far optical fields. The nanostructured metal-dielectric interface with confined SPs such as the dark modes contributes to constant amplification of stimulated emission of the SPs without radiation and increases the SP population. It resembles an optical cavity with two reflectors with 100% reflectivity allowing light to bounce back and forth when passing through the gain medium. As a result, a high Q factor is achieved due to the dark modes. If these dark modes are partially converted into luminous modes, which can be achieved by breaking the symmetry of the plasmonic nanostructures [18], resonance amplification at the optical frequencies by stimulated emission of radiation fueled by SPs is accomplished simultaneously resulting in lasing of coherent light.

The Q factor characterizes the quality of the resonant cavity in the laser device. As aforementioned, a plasmonic nano-laser is different from a conventional laser in that the diffraction limit of the effective mode forces the Q factor to be extremely high. The Purcell factor, which regulates the spontaneous emission coupling, is affected by localized confinement which relies on the ratio of the Q factor to mode volume [19]. In plasmonic devices, the plasmon modes

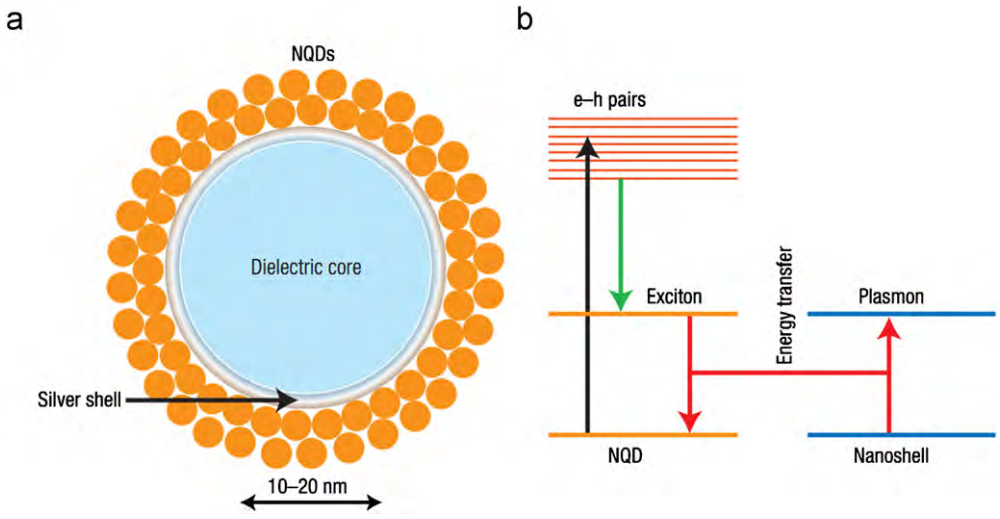

Figure 1 (a) Schematic of a spaser made of a silver nanoshell on a dielectric core and surrounded by two dense monolayers of nanocrystal QDs; (b) schematic of the levels and transitions in a spaser [17].

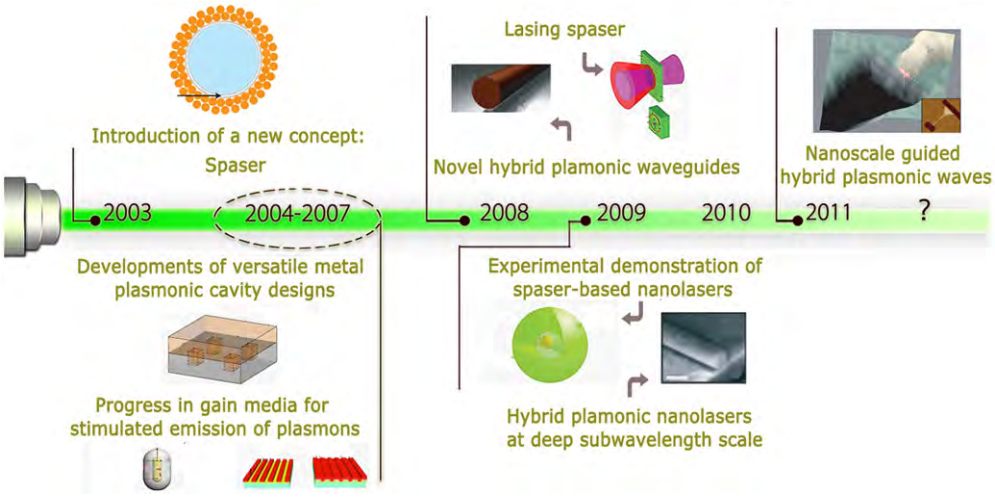

Figure 2 Recent progress in plasmonic nano-laser systems.

have mode volumes that break the diffraction limit, and thus a high Purcell enhancement as well as good confinement factor can be achieved in spite of a smaller Q factor. Therefore, operation of a plasmonic nano-laser with a small Q factor is possible. For instance, a low-threshold or no-threshold laser can be achieved due to the high Purcell enhancement because preferential emission may be coupled to a special lasing mode to further enhance the efficiency of stimulated emission [20]. Ultrafast generation and amplification of SPs for lasing can be modulated at frequencies up to terahertz on account of the Purcell enhancement. Despite limitation by the metal absorption loss, the plasmonic modes have a broad band and enhance emission over a large bandwidth [14].

In this review, we focus on the more recent developments (~8 years) in the area of plasmonic nano-lasers and discuss the general guidelines for device design (Fig. 2). Recent results indeed demonstrate that a plasmonic nano-laser can effectively overcome many of the difficulties and limitations in plasmonics and the technique has immense potential in sub-wavelength photonic circuits and single-molecule exploration. Because this technique is relatively new, future challenges and research directions will also be discussed.

Loss in metal plasmonic resonant cavity

A resonant cavity is a critical part of a laser device. It determines the mode and direction of the light beam (or coupled light beam in a plasmonic nano-laser), and the feedback energy is provided by the light bouncing around in the cavity. Cavities constructed by photonic crystals with confined localized dimensions on the same order of the wavelength in each direction have been theoretically shown [6,21,22]. The photonic crystal cavity can yield a high Q factor, but the effective mode volume has a lower bound constraining the Purcell enhancement. Hence, there are challenges in sub-wavelength confinement as well as large-area and broadband enhancement. In this respect, plasmonics has paved the way for the design of a micro- or nano-scale cavity approaching the diffraction limitation. The Q factor, denoting the quality of a cavity, is crucial to a traditional laser resonator, and it is the same for a plasmonic nano-laser. In the latter case, the resonant cavity refers to a micro- or nano-cavity formed by metal nanostructures where resonant excitation amplification of plasmons takes place.

Resonant micro- or nano-cavities fabricated by metal nanostructures confine the EM energy within the sub-wavelength volume, but there is heavy intrinsic loss of the localized plasmon energy during propagation, especially at the optical frequencies. It is mainly due to the large scattering loss, dissipation loss arising from absorption, and radiation loss because of unexpected coupling. Scattering loss due to roughness, domain discontinuity, and defects increase dissipation of the confined energy [23]. Furthermore, micro- or nano-scale metal structures with complex permittivity in which the imaginary part results in energy damping further induce loss in the propagation of plasmons. Although the plasmons exhibit strong modal confinement forbidding far-field radiation, there is still unwanted coupled radiation precluding effective mode conversion and energy propagation. Therefore, losses in a metal micro- or nanocavity degrade long-range plasmon propagation and severely affect low-energy-loss SPP propagation in a plasmonic nano-laser.

Excitation and propagation of plasmons on metal films

Metal cavities with a compact volume on the micro- or nano-scale exhibit inefficient plasmon excitation and appreciable energy decay resulting from electron collision and emission of elastically scattered photons from the rough metal surface, defects, and domain boundaries. On the other hand, at the boundary between a dielectric and metal, incident light (visible and infrared frequencies) exhibits SP resonance and provides the necessary conditions for phase matching of the collective electron oscillations. It should be noted that the resonance frequency of SPs as well as SPP propagation is extremely sensitive to interface environment and properties such as size, shape, and materials. Therefore, by adopting the appropriate nanofabrication techniques, the desirable surface topography, size, and geometry can be produced so that metal nanostructures can be used as effective plasmon propagation cavities to deliver efficient

SP excitation and propagation of SPP with lower energy dissipation. Both are crucial to photonic integrated circuits and devices.

The wave vector of the SPP is obtained by solving Maxwell's equations at the planar metal-dielectric boundary:

$$k_{SPP} = k_0 \left(\frac{\varepsilon_1 \varepsilon_2}{\varepsilon_1 + \varepsilon_2} \right)^{1/2} \quad (1)$$

where k_{SPP} is the wave vector of the SPP, k_0 is the wave vector of the incident EM wave, and ε_1 and ε_2 are the permittivity values of the dielectrics and metal, respectively ($|\varepsilon_2| > \varepsilon_1$ and the real part of $\varepsilon_2 < 0$). Considering the relationship between the wave vectors of the incident light, reflected light, and transmitted light, the wave vector of the SPP is always larger than that available to the incident plane waves in the adjacent dielectric medium. The dispersion curve of the SPs always lies outside the light cone and therefore, plane light waves cannot excite the SPP directly.

In order to enhance the efficiency of SPP excitation, an attenuated total reflection setup has been proposed to generate collective electron oscillations and detect the propagation of SPP [8]. Using a prism in an attenuated total reflection arrangement on glass attached to a metal film, an incident light beam with angles below the total internal reflection contributes to an evanescent wave with a wave vector that may match that of the propagating SPP at the metal/air interface. Noble metal films are promising in the guiding and propagation of plasmons [24] and metal films with simple structures can also be easily attached to the devices for effective plasmon excitation.

In these setups, energy loss still occurs as the plasmons propagate back into the prism. Thicker metal films can mitigate such energy loss, but there are concomitant side effects. For example, an evanescent wave with a wave vector that may not match that of the SPP leads to failure in SP excitation [8]. In addition, as a means of far-field collective excitation, the excitation area and measurement area should be separated. Since the highly localized electron oscillations are confined, SPP propagation is supposed to occur outside the excitation region without interference by unexpected light modes. Slight modulation of the attenuated total reflection prism and use of well-designed metal films have been proposed to lower the energy loss and increase the propagation length of SPP. Lamprecht et al. developed a metal waveguide using thin Au and Ag films containing stripes with micrometer widths (1–54 μm) and investigated the propagation of localized SPs along the cavity [25]. In this setup, an opaque aluminum screen provided the separation between the plasmon excitation and propagation areas (see Fig. 3(a)). The tilted geometry of the metal stripes crossing the Al film was believed to give rise to the enhanced effective plasmon excitation. The SPP propagation length as a function of Au and Ag film stripe widths has also been measured. Fig. 3(b) illustrates that the SPP propagation length decreases with reduced Ag stripe width below 20 μm. As the width is reduced, plasmon scattering from the side increases, thus leading to energy damping and smaller propagation length. Weeber et al. used a photon scanning tunneling microscope to observe the SPP modes on thin film

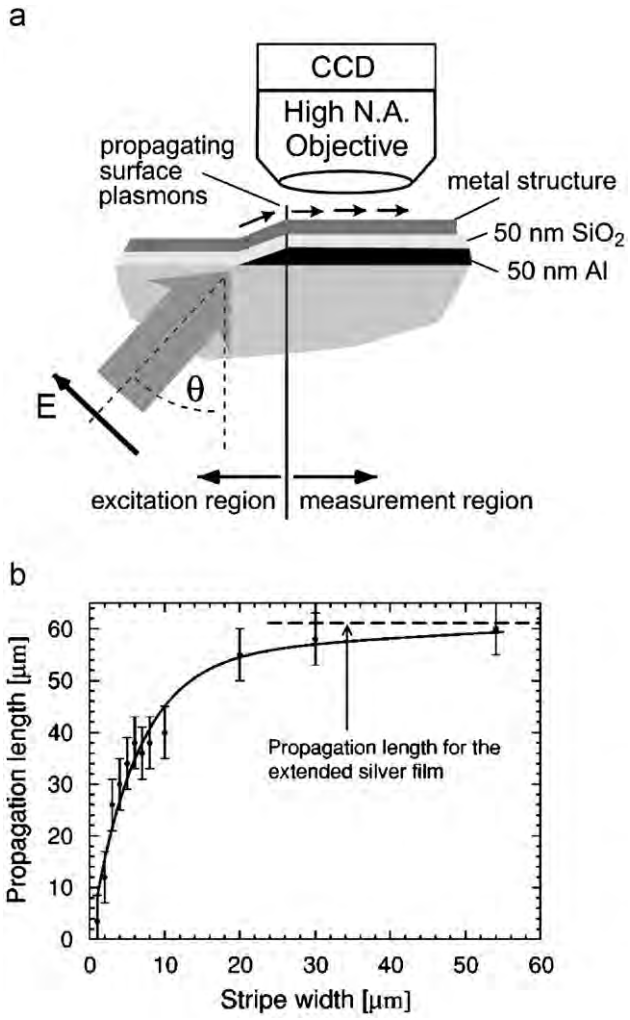

Figure 3 (a) Schematic of the experimental setup of spatially confined SPs excitation; (b) experimentally obtained SPPs propagation length in 70-nm-thick silver stripes versus stripe width [25].

stripes with widths of 2.5 and 3.5 μm at a visible frequency [26]. These stripes which support long-range SPP may provide a good means to develop noble integrated optical cavity devices.

Plasmonic band-gap nanostructures fabricated on thin metal films have recently been used as nano-cavities to accomplish lasing with highly efficient SP resonance excitation [27–30]. The SPP wave vector is always larger than that of the incident plane waves and so it is difficult to excite SPP directly on a planar metal surface by plane waves. However, it can be remedied using corrugated metal films with grating grooves (see Fig. 4) [31–35]. A grating vector introduced by the corrugated structures makes it possible to match the wave vector of the SPP. In addition, the lower velocity of the SPs due to the wide plasmonic band gap of the nanostructures reduces the lasing threshold [36]. Okamoto et al. have theoretically analyzed the metal absorption loss at the band gap edges of 1D rectangular periodical corrugations in thin silver films by the coupled-wave approach [27]. Based on their findings, the behavior of plasmonic lasers with 2D band gap structures can be predicted.

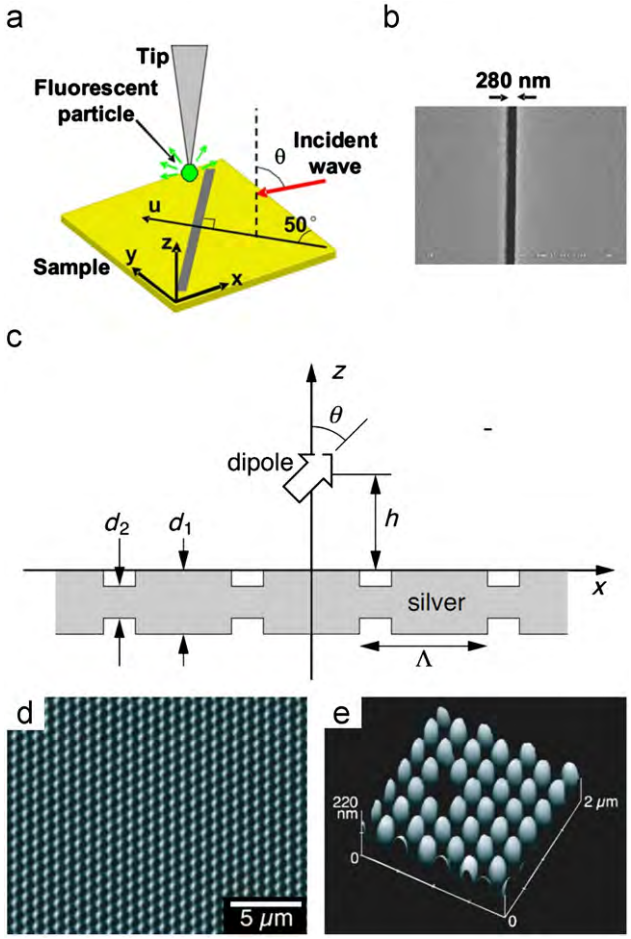

Figure 4 (a) Schematic of the experimental configuration of the metal film silt with a 50° angle to the *x* axis; (b) SEM image of the slit [35]; (c) schematic of the corrugated metal thin film structures [30]; (d) SEM image of the fabricated 2D grating on photoresist; (e) scanning AFM image of a metal grating including a point defect on the photoresist [27].

Enhanced plasmonic coupling among metal inter-nanoparticles

Resonant excitation of SPs in noble metal nanostructures is linked to their size and shape [37]. As metal nanostructures become smaller, they exhibit strong local SP enhancement of collective electron excitations without radiation [38–40]. Because of strong near-field interactions between adjacent particles, the localized SPs can couple to the SPP modes with energy transferred between these plasmonic nanoparticles. This suggests the possibility of efficient concentration of SPs and reduced energy loss to enable SPP propagation along a larger distance.

The smaller loss and larger enhancement arising from neighboring particles lead to excellent energy confinement. However, integrated plasmon waveguides with metal nanoparticles have difficulty in modulating large energy propagation lengths. It has been shown that finite metal nanoparticles chains can effectively transport EM energy by excitation of near-field localized plasmons in the periodic arrays [41,42]. Zhang et al. have investigated the plasmon resonance peak wavelength of finite chains with Au nanoparticles as functions of chain length as well as particle size and spacing [43,44]. Theoretical analysis of the energy propagation in plasmonic waveguides consisting of metal nanoparticle chains has been conducted using the dipole coupled approximation model [42,45–49]. Assuming that the energy transport through the metal nanospheres linear chains is caused by the near field, Brongersma et al. investigated the optical bandwidth dependence on the energy splitting between the longitudinal and transverse polarized dipole resonances [42]. Calculations based on the coupled dipole approximation illustrate that the propagation direction can be bent by 90° by altering the particle size, spacing, and index of the surrounding medium [47]. In Markel's works [49], two types of SPs were identified from the linear chains of metal nanoparticles by computer simulation and dipole coupled approximation: ordinary (quasistatic) and extraordinary (nonquasistatic). The spatial energy decay caused by absorption and radiative dissipation is quantitatively attributed to Ohmic loss in the metal and disorder in the chains.

Maier et al. conducted far-field excitation measurements to examine the near-field inter-particle coupling action and plasmon propagation in Au nanoparticle plasmonic waveguides [50]. Particles produced by electron beam lithography on indium tin oxide coated glass were periodically arrayed. The energy splitting between the longitudinal and transverse collective mode excitations of the SPs with different numbers of nanoparticles is consistent with theoretical analysis by the dipole coupled approximation model. The energy loss in plasmon waveguides can be estimated based on the far-field measurements and information regarding to the peak energy splitting and homogeneous linewidth of the collective oscillations can be obtained. Both the nearest-neighbor interactions and second nearest-neighbor interactions are required to properly describe the SPP propagation. The simulation results yield an estimated energy loss of 3 dB/130 nm and propagation length of 370 nm. It also indicates that using metal nanoparticles with the right size, geometry, and materials type in the plasmonic cavity, optimized plasmon waveguides can be produced to guide the EM energy (SP resonance) over a large distance with small energy loss.

Investigations have, however, been limited to collective excitations of SPs in plasmonic waveguides. It is challenging to investigate energy propagation along the cavities due to the lack of experimental methods. Since SPs are excited by highly localized electron oscillations, they have to be confined to an area away from the propagation measurement region. The advantages of near-filed SPs excitation in experimental propagation measurement outweigh those of far-field excitations, which are dominated by collective excitations of particles. Maier et al. have used a scanning near-field optical microscope to provide direct near-field excitation of SPs on individual Ag nanoparticle of a metal chain in plasmonic waveguides [51]. The energy transport is studied using fluorescent nanospheres attached to the top of nanoparticle chains as shown in Fig. 5. If the distance between the tip and fluorescent nanospheres is sufficiently large, dye emission accompanied by energy propagation results. In fact, direct evidence of SPs propagation over a distance of 500 nm has been demonstrated on a nanosphere placed on the plasmon waveguide.

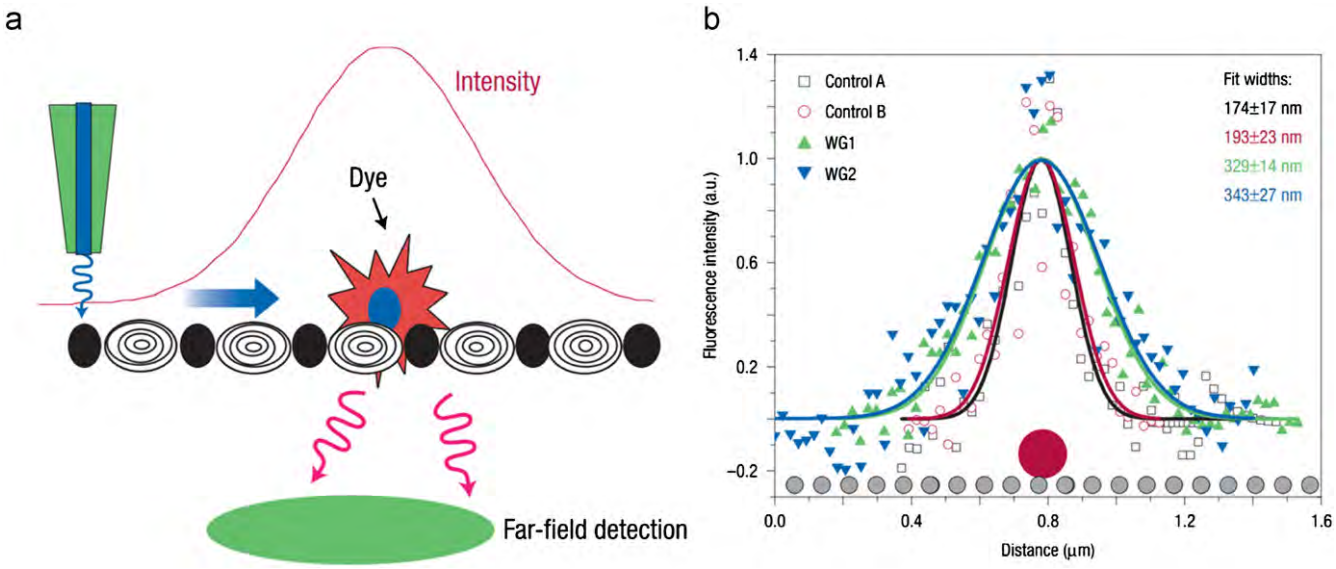

Figure 5 (a) Schematic of a plasmonic waveguide of the near-field excitation by scanning near-field optical microscopy. The waveguide transports the EM energy to a fluorescent nanosphere and the fluorescence intensity for varying tip positions is collected in the far-field; (b) evidence of energy transport in plasmon waveguides by the width of the intensity of fluorescent nanospheres and Gaussian line-shape fits to the data show an increased width for nanospheres located on the plasmon waveguides [51].

Plasmonic nanowire-cavity

Metal nanowires with the proper dimensions and materials have been used in surface plasmonic cavities to optimize energy propagation and reduce loss. In this type of surface plasmonic resonator, SPs are reflected from the wire end. If the integer value of half of the coupling wavelength of the SPs is equal to the wire length, plasmon modes exist in the resonator and traverse along the nanowire axis [52,53]. Excitation of the SPs in the metal nanowire cavity is accomplished by either uniform illumination of an optically coupled total internal reflection prism or a focused local near-field probe. The intensity of the photons arising from elastically scattering at the distal end faces of the wire reveals the SPP propagation behavior [23,54,55].

Scattering and collisional losses are observed from rough surfaces, domain discontinuities, and defects because they disrupt energy propagation. Recently, Ag nanowires in a plasmonic resonator with a well-defined crystal structure have been shown to reduce the SP energy loss [23]. The plasmon wave modes with a wavelength of 414 nm are compared to the excitation laser with a wavelength of 785 nm. The wavelength ratio reveals that the plasmon modes are not coupled to the far-field light in air or on the substrate, and so there is no radiation loss during energy propagation along the nanowire resonator. Accordingly, a large propagation distance of 10 μm is observed from the nanowire plasmon resonator that is 18.5 μm long. In comparison, chemically prepared Ag nanowires exhibit better plasmon propagation than lithographically fabricated ones. Dickson et al. studied the lengths of plasmon propagation in metal nanowires composed of Au and Ag and the propagation behavior at excitation wavelengths of 532 and 820 nm [55]. Their experiments disclosed substantially longer plasmon propagation lengths in both metals at 820 nm excitation as well as better performance of Ag than Au at both wavelengths (see Fig. 6(a)–(e)). In general, SPPs propagating freely along the metal surface make it difficult to achieve directional emission and obtain the necessary cavity feedback for lasing. Unidirectional SPPs propagating over a distance of 10 μm have been achieved from a bimetal wire with a sharp Au/Ag heterojunction. As shown in Fig. 6(f)–(h), emission of scattered SPs wave is observed only from the Ag end of the wire. The Au tip illuminated by 820 nm light shows no observable emission.

Gain in plasmonic emission

Collective electron oscillations are coupled to SP modes on nanostructured metal surface so that the energy can be concentrated in the plasmon resonant cavity to overcome the diffraction limitation. SPPs propagate along the interface, but reduction in the direction perpendicular to the surface may induce high absorption losses and decrease the propagation length, especially in close proximity between the confined plasmon modes and metal layers. A micro- or nano-cavity consisting of metal structures has a negative complex permittivity. The negative real component of the complex permittivity coexists with the imaginary part, and the localized SP resonance and plasmon propagation are affected negatively. At visible frequencies, a metal surface is an imperfect conductor that produces resonance losses such as Ohmic loss. Reduction of metal absorption loss and compensation for the propagation length degradation in a plasmonic cavity depends on a dielectric medium which provides the gain surrounding the metal nanostructure. When there is coupling between SPP modes and materials, the metal damping loss can be compensated and SPP propagation will be enhanced.

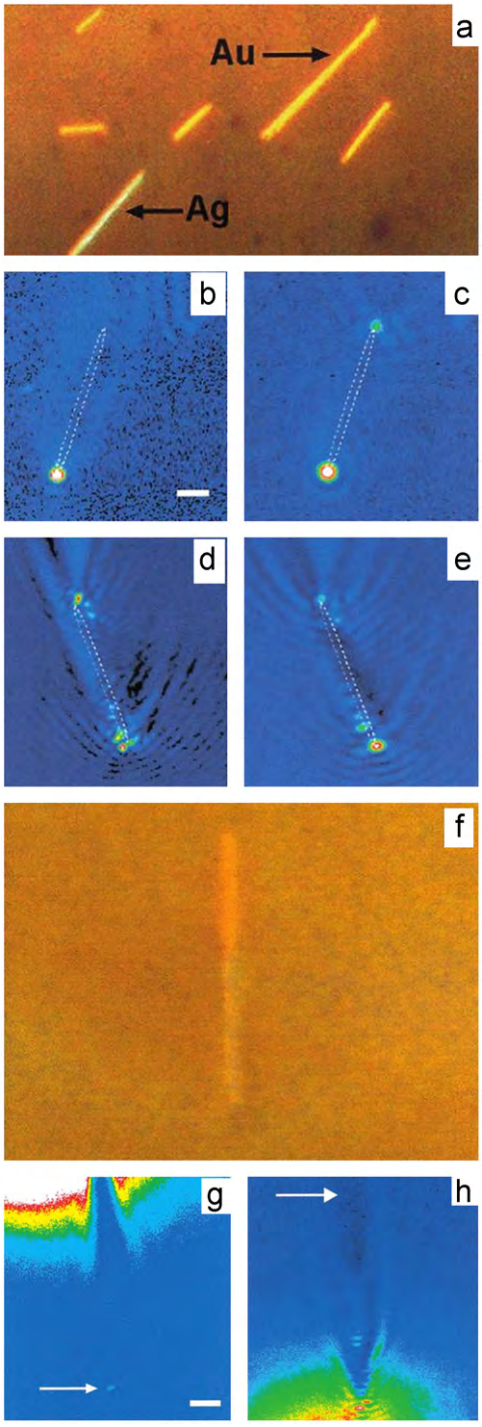

Figure 6 (a) Au and Ag nanorods used for the plasmon propagation experiments; (b) optical microscope image of a 4.7 μm long Au rod exposed to the illumination at 532 nm with accordingly strong scattering at the rod input and the absence of scattering at distal tip. (c) Same Au rod under illumination at 820 nm, and both ends of the rod exhibit strong emission/scattering; (d) and (e) a 4.7 μm long Ag rod illuminated at 532 and 820 nm, respectively; (f) a bimetal Au/Ag rod. The upper 40% of the rod is Au while the remainder is composed of Ag; (g) the Au end of the rod shown in panel (f) under illumination at 820 nm; (h) Illumination at the Ag tip by 820 nm with no emission from the Au tip is observable [55].

Gain assisted localized plasmons compensation

A semi-infinite gain medium theoretically exhibits amplification with a critical gain and contributes to a singularity in the localized SP resonance of the single metal nanoparticle structures [56,57]. The singularity in metal nanospheres arises from slashing the imaginary part and promotes the local field enhancement factor, which is $\propto(\varepsilon_d-\varepsilon_m)/(2\varepsilon_d+\varepsilon_m)$, where ε_d and ε_m are complex dielectric constants of the dielectrics and metal, respectively. Enhancement of the localized SP resonance is indicated by an increase in the Rayleigh scattering within the plasmon band. In particular, six-fold enhancement has been observed from metal nanoparticles mixed with a dielectric medium of Rhodamine 6G dyes. The gain attained compensates the metal absorption loss [58,59]. It is achieved when resorting to the optical gain in the dielectric medium surrounding the metal nanostructures. Since the interactions between the dye molecules and metal nanostructures may lead to resonant energy transfer from the fluorescent molecules to the SPs, molecules such as Rhodamine 6G dyes are always placed in close proximity to the metal nanostructures for localized SP resonance [60–63]. In the presence of the gain molecules, considerable enhancement in the Q factor in SP resonance can be achieved.

Luca et al. have prepared a gain-functionalized metal plasmonic nanostructure [64]. The smart gain-functionalized composite is different from conventional gain-assisted systems in which metal absorption losses remain unresolved. Instead of randomly dispersing fluorescent guest molecules in a solution with metal nanoparticles, dye molecules are encapsulated into shells. The built-in gain elements intended for compensating internal losses are obtained by incorporating the optically active gain component of Rhodamine 6G dye molecules into the silica shell surrounding the metal nanoparticles. The nonradiative excitation energy transfer from the fluorescent dye molecules to SP resonance has been demonstrated. A comparison of the modified Rayleigh scattering and transmission as a function of pumping energy between the gain-assisted and gain-functionalized plasmonic nanostructures is shown in Fig. 7. The results provide experimental proof that gain media, which are properly inserted into metal plasmonic nanostructures functionalize the gain unit for strongly absorbing metals.

Near-field strong interactions between neighboring plasmonic particles provide highly enhanced localized EM field and excellent subwavelength energy confinement. This is a potential way to concentrate the energy. However, energy damping along the SPP propagating path due to metal absorption can reduce the propagation length. Therefore, SPPs propagation with good confinement as well as small energy loss is necessary in order to produce subwavelength plasmonic waveguides integrated with metal nanoparticle arrays [65–70]. It has been demonstrated that a gain medium in metal nanoparticle arrays can enhance the propagation length of the SPP and reduce the energy loss [71–73]. Citrin theoretically studied the benefits of embedding optical gain media in nanoparticle chains to offset the energy loss [72]. In the presence of a gain medium, exponential increase in the plasmon modes can compensate for nonradiative damping of the SP resonance decay. The dispersion equation governing

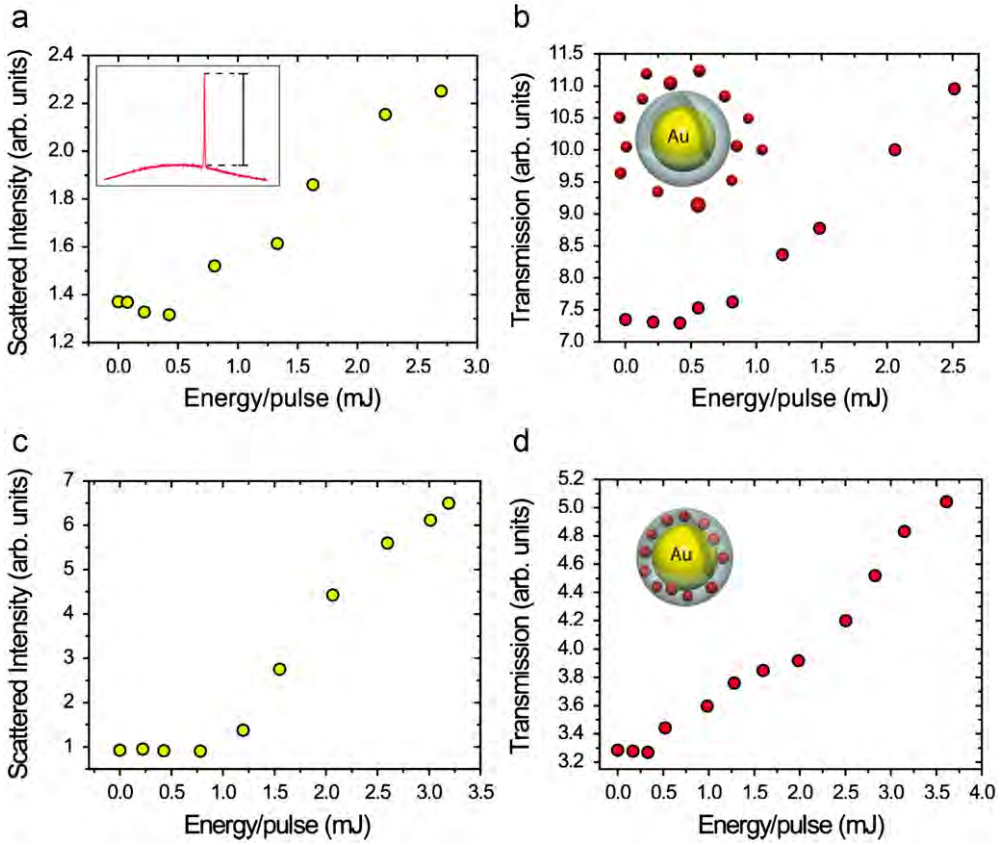

Figure 7 Comparison of Rayleigh scattering and transmission enhancement signals between gain-assisted (a, b) and gain-functionalized (c, d) samples [64].

gain-assisted SPPs in linear metal nanoparticles and the associated propagation characteristics of nonradiative SPPs have been presented and discussed [73]. Ohmic losses are nearly compensated by the gain in the host medium. Besides, the gain medium has a large influence on the transversely polarized SPs and forces them to decay on longer scales compared to the longitudinally polarized ones.

Plasmonic semiconductor quantum gain

Fluorescent molecules close to the interface of metal nanostructures can compensate for the energy loss of SPs including intrinsic metal absorption loss and external radiative loss. Unfortunately, although fluorescent dye molecules yield strong photoluminescence and reduced intrinsic loss, they oxidize easily and tend to bleach. It is possible to increase the molecular concentration to offset the energy loss in metals. However, emission quenching in fluorescent dyes accompanies coupling of dye emission to the SP modes. On the other hand, in plasmonic lasing, a high Purcell enhancement in the cavity can be achieved by a small Q factor because the mode volume can be confined below the diffraction limit. Nevertheless, a small Q factor imposes a high demand on the active regions of the gain medium in order to compensate for the large loss. Fluorescent dyes decay easily because of spontaneous radiation into free space, excitation of the electron-hole pairs in the metal, and unexpected SP modes outside the nanostructures. The decay rate can be lowered to that of stimulated emission, but this imposes stringent requirements on the emitters to lase at a lower threshold. Additionally, in plasmonic nano-laser systems with dye gain, electrical contacts are difficult to implement. It is because the organic dye molecules cannot be incorporated in an efficient and stable manner using existing technology especially at room temperature.

Semiconductors have been suggested to guide SP waves in metal subwavelength nanostructures beyond the diffraction limit. A semiconductor serving as the gain medium pumped *via* electrical injection has been proposed and the semiconductor nanostructures can serve as both the gain media and waveguide [74,75]. The confinement factor is boosted due to the large overlap between the electronic and photonic modes. Lasing from semiconductors depends on photonic waves instead of plasmonic waves. Since the wavelength of the latter is orders of magnitude smaller than that of the former ones and inevitable diffraction limit, the lasing source cannot reach the subwavelength dimensions. Besides, as the size of these miconductor nano-laser decreases, the confining and guiding of modes lead to inefficient amplification and a higher threshold. As a result, metal plasmonic nanostructures containing a semiconductor active gain medium have better prospects in nanoscale lasing. A semiconductor with a sufficient carrier density can be stimulated by electron injection or external optical pumping. Both the intrinsic and raditive losses in the SP

resonance can be mitigated and the localized EM modes increase the performance of other nano-lasers.

Theoretically, some concepts and definitions have been reexamined for novel plasmonic lasing devices with a semiconductor as the active gain medium. Li and Ning proposed the concept of a confinement factor for a metal-semiconductor-metal waveguide near SP resonance [76,77]. The SPP modes exhibit an unexpected giant modal gain, which is thousands of times larger than the materials gain. Therefore, the large ratio of modal gain to materials gain contributes to a large confinement factor. Hill et al. have used a semiconductor core as the electrically pumped active gain medium and conducted metal encapsulation [78,79]. The metal-insulator-metal waveguide is observed to reach 1D mode confinement below the diffraction limit. Here, the cryogenic temperature required for lasing offsets the large resistive loss from metal absorption. There is less Auger recombination under cryogenic conditions and so a larger Q and lower threshold can be obtained.

Although wavelength compression of SP modes into the nanometer scale is attractive for nanoscale plasmonic lasing devices, the effective minimum wavelength affects the metal absorption losses. Near the SP resonance frequency, the SP modes experience significant absorption losses when propagating along the metal interfaces [9,80]. To make things more complicated, although SP resonance provides superior localization, the small volume of the laser device forces the propagation of SPP to be highly confined in the very small region of the metal interface further hindering efficient gain compensation. When the emitting frequency is high, the carrier injection energy in the semiconductor goes in the positive direction but in the metal, it goes in the opposite direction. The opposite effects make the net gain almost zero. Recently, Stockman analyzed full compensation (overcompensation) [81]. The instability of the transition to a lasing state further limits loss compensation.

Quantum treatment of SPs has been theoretically proposed to analyze the gain conditions and laser operation in plasmonic systems [82–84]. As an active gain medium formed by the two-level emitters, the operating frequencies of the semiconductor quantum structures can be modulated to transfer energy into the desired spectral range. This is accomplished by engineering the geometry of the metal plasmonic nanostructures. They also offer good quantum confinement, large packing density, high transition efficiency, as well as narrow transition lines and the frequency is tunable [85]. Stockman introduced a quantum generator for SPs by incorporating semiconductor quantum dots as the emitter and laser active medium and theoretically demonstrated the mechanism of spaser [7]. PbS QDs incorporated into polymer films adjacent to gold nanofilms have been used as the amplifying medium to increase the propagation length by 30% [86]. Semiconductor quantum wells have also been widely used since current quantum well technology is capable of compensating intrinsic SP attenuation even near the plasmon resonance and lengthening SPPs propagation. Ambati et al. investigated the emission phenomenon of an optical emitter into various channels of SPs [87]. The active planar metal-film system comprises InGaN/GaN and a silver film and coupling between the SP modes and gain medium can be precisely controlled by strategically positioning the emitters.

Stimulated emission of plasmonic modes

Although the well confined near-field of the SP modes may not allow coupling to the far zone optical field, SPs can achieve amplification and radiation when combined with an active molecule gain medium. This is because the molecule is only affected by the field at the specific position regardless of the overall symmetry of the entire local field. Seidel et al. observed stimulated emission of SPs at the interface between a thin film and an optically pumped dye solution [88]. Stimulated emission of SPs from dye-doped polymeric microcylinder cavities deposited on gold and silver wires was observed [89]. Noginov et al. added aggregated silver nanoparticles to a Rodamine 6G dye solution to enhance the efficiency of spontaneous and stimulated emission [90]. However, the feedback mechanism is still not well understood. Nanoparticles with a gold core and dye-doped silica shell were employed to demonstrate resonant energy transfer from excited molecules to SPs and stimulated emission of SPs in the luminous mode [16]. The absorption loss of localized SPs in gold nanoparticles is sufficiently offset by the active gain in the plasmonic nanosystem. Coupling of the stimulated emission of the SP modes to photonic modes at a wavelength of 531 nm was experimentally confirmed and the mechanism was studied. Fig. 8(a)-(c) depicts the stimulated emission spectra of the nanoparticle sample at different energy pumping. When the pumping energy is low, emission is barely observed because there are no excited gain molecules to transfer energy to the SP modes (spectra 4 and 5). As the pumping energy is increased, emission occurs. If the pumping energy is increased to the critical threshold value, the stimulated emission of SP resonance becomes intense. If the sample is diluted more than 100 times, the emission intensity decreases but the spectral characteristics do not change. This demonstrates that the stimulated emission of SPs is produced by single nanoparticles, rather than collective stimulated emission effect in a volume of the gain medium.

Energy losses in the SP modes can be balanced by introducing active gain media into the metal structures. Efficient coupling to the plasmon modes lowers the plasmon lasing threshold and aids in the formation of high-efficient coherent radiation. Therefore, a good understanding of the fundamental interactions between SPPs and gain medium enables wide applications on nanoscale plasmonic lasing sources [91]. Unfortunately, the process is rather complex. Efficient energy transfer from the gain medium to SP modes contributes to spontaneous emission which is important to the expected coupling modes and initiation of stimulated emissions of SPs. In the case when the pumping intensity is very high, the competition between stimulated plasmons emission and amplified spontaneous emission affects the SPPs propagation and undermine coupling to the plasmonic modes. Therefore, amplified spontaneous emission of SPs limits the gain compensation for loss with regard to SPP propagation. It is similar to that in a conventional laser. Recently, a new class of SPs amplifier benefiting from the reduced spontaneous emission may provide low-noise optical amplification and large loss compensation [92]. Many energy decay channels have been revealed based on the reduced spontaneous emission. Fig. 8(d) depicts the main energy decay channels for long-range SPPs amplication with

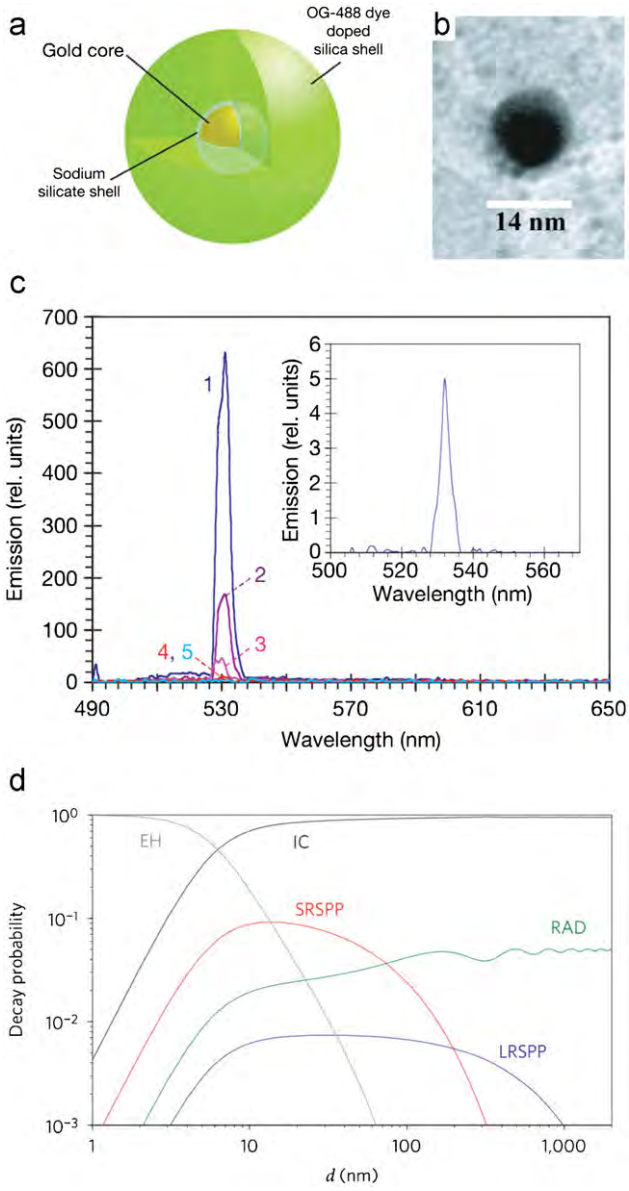

Figure 8 (a) Sketch of the hybrid nanoparticle architecture (not to scale) with dye molecules throughout the silica shell; (b) transmission electron microscope image of Au core; (c) stimulated emission spectra of the nanoparticle sample pumped with 22.5, 9, 4.5, 2, and 1.25 mJ. Inset: stimulated emission spectrum at more than 100-fold dilution of the sample [16]. (d) Decay probability of isotropically oriented dipoles near a metal slab into various channels [92].

optically pumped dye molecules as the gain medium. The decay probability depends on the distance from the metal and dipole moment orientation. Spontaneous emission coupled to the radiation modes prevents it from coupling with long-range SPPs near the metal. While spontaneous emission occurs close to the metal interface, the probability of coupling to radiative modes is considerably reduced. Owing to the larger modal loss, short-range SPP hardly contributes to the emission output. In addition, metal absorption couples energy into electron-hole pairs thus leading to fluorescence quenching and reduced spontaneous emission. By carefully engineering the active plasmonic systems with the proper gain medium, efficient coupling to the desirable SP modes can be achieved to get rid of the unwanted emission modes and reduce the thresholds for plasmonic lasing.

Hybrid long-range plasmonic laser

Long-range SP waves have been observed from thin metal films [93] and there is much interest in the traveling modes due to advantages such as small propagation loss and relatively long SPPs propagation length [94–97]. When thin metal films are bounded by identical dielectrics on both sides, field tunneling through the metal causes the plasmon modes to form two kinds of coupled SPPs, namely long-range SPPs and short-range SPPs. The former arises from the symmetrical spatial charge distribution across the waveguide between the top and bottom surfaces. The fields are screened by the metal to reduce the effect of absorption and increase the propagation length. When anti-symmetrical charges are distributed, short-range SPPs are produced [98]. By varying the frequencies of the incident light, different surface charge density distributions can be generated for long-range SPPs propagation. Moreover, by modulating the geometric configuration of the metal films, optimized long-range SPPs propagation with low energy loss can be achieved. Berini analyzed long-rang SPP modes in waveguides consisting of thin metal films with different widths and thicknesses [99–101]. A propagation length hundreds of times longer than that of the single-interface in the corresponding plasmonic structure was disclosed.

Gain-assisted long-range SP modes, which provide efficient energy transfer to offset intrinsic propagation loss, have drawn considerable attention. The efficiency of coupling energy from excited fluorescent molecules to long-range modes has been theoretically calculated using the rigorous coupled wave approach on corrugated metal thin film structures, which otherwise support only short-range SP modes in the absence of gain compensation [30]. A dipolar gain medium was adopted for the amplification of long-range SPs in a symmetrical metal film waveguide where optically pumped Rhodamine 6G dye molecules were incorporated as the gain medium [102,103]. Gather et al. observed active gain enabling plasmonic propagation of long-range SPP modes over macroscopic distances [104]. The gain was provided by an optically pumped fluorescent layer adjacent to the metal surface in a dielectric–metal–dielectric plasmonic waveguide. By measuring the spontaneous emission in a long-range SPP mode, the net gain could be derived quantitatively. In fact, efficient energy transfer from the gain medium to SP modes is important to the expected coupling modes, which initiate stimulated emissions of SPs. The results also show that when the amplified spontaneous emission threshold is reached, amplification of the SP polaritons is dominated by the spatial overlap of the confined plasmonic modes and gain medium.

SPs waves are highly concentrated in a very small region of the metal–dielectric interface and as a result, large gain requirements are imposed by the complex interfaces. They restrict the gain amplification process and make it even more difficult for plasmon modes to overlap the active gain

medium. Operation at frequencies much lower than the SP resonance frequency is widely adopted. One of advantages is that the plasmon modes are not strongly confined to the metal surface and can therefore overlap with the active gain structures [105–108]. Genov et al. demonstrated that by keeping plasmon modes away from the resonance frequency, the light–matter interactions in the plasmonic systems can be increased in two dimensions [109]. However, this does not bode well for localized confinement. Long-range SPPs exhibit optical confinement which is comparable to that of conventional dielectric waveguides and so they cannot reach the subwavelength dimensions.

Tight confinement of the EM energy affects the energy loss in the coupled optical field on the metal side of the interface. By reducing the spatial distribution of the SPP modes in the nanostructures, good confinement can be attained, but it causes more metal absorption and energy loss. Nezhad et al. produced optically pumped metal–dielectric cavities comprising a metal bilayer surrounding an InGaAsP disk as gain medium [110]. By increasing the diameter of the gain disk, the optical mode was not observed from the metal surface in addition to reduced resistive loss. Although the cavity size is smaller than the emission wavelength in all three dimensions, the diffraction limit remains because of the nature of the photonic modes instead of plasmonic ones.

A hybrid approach to increase the EM field from the metal to the dielectric gap was introduced to achieve optical gain in plasmonic waveguide with subwavelength confinement and overcome the high resistive loss experienced in the long-range SPPs propagation in the metal especially at visible and near-infrared frequencies [20,111,112]. Fig. 9(a) shows the hybrid optical waveguide which consists of a high index semiconductor nanowire on top of a metal substrate separated by a thin low-index insulator. By tuning the geometrical properties of the structure such as the cylinder diameter d and gap width h, coupling between the optical mode of the dielectric waveguide and SP modes at the metal–dielectric interface increases the propagation distance of the hybrid plasmonic modes to millimeter ranges with smaller loss while retaining a moderate degree of confinement. As shown in Fig. 9(b), the hybrid waveguide with a large cylinder diameter and gap width supports a low-loss cylinder mode, which is well confined to the high-permittivity dielectric core. When the diameter of the cylinder is decreased, mode coupling results in a new hybrid mode that features both the cylinder and SPP characteristics. The hybrid modes distribute over both the cylinder and the adjacent interface of the metal–dielectrics (see Fig. 9(c)). With regard to the reduced gap widths (Fig. 9(d) and (e)), the hybrid mode is confined in two dimensions in the gap and does not exhibit the characteristics of either the cylinder or SP mode. Furthermore, the hybrid long-range SPP mode supports strong confinement to sizes of more than 100 times smaller than the diffraction limited spot in two dimensions with low propagation loss. In other similar plasmonic waveguides, the SPP waves in the dielectric–metal interface are only confined in one dimension.

This type of hybrid plasmon waveguide allows long-range SPPs propagation with high subwavelength confinement and small resistive loss in the metal especially at visible and near-infrared frequencies. A plasmonic laser (see Fig. 10(a)) with the deep subwavelength scale based on the hybrid plasmonic waveguide has been experimentally demonstrated [20]. The hybrid plasmon modes in the insulator gap overlap with the semiconductor gain and mitigate the high resistive loss in SPPs propagation. The hybrid plasmonic waveguide also enables energy storage in the insulator gap regions. The plasmonic nature of the confined modes in this hybrid waveguide has been assessed based on the broadband enhancement of the exciton spontaneous emission rates. Fig. 10(b) shows the laser oscillation in the hybrid waveguide. The onset of amplified spontaneous emission is observed at a moderate pumping intensity of 10–60 MW cm^{-2} (see Fig. 10(c)). When the input energy is increased, nonlinear response is observed from the integrated output power. It demonstrates that a high pumping power provides sufficient materials gain to achieve increased cavity mode resonance and full laser oscillation. This noble hybrid plasmonic nano-laser not only allows deep subwavelength detection, but can provide a convenient method for electrical injection in optoelectronics.

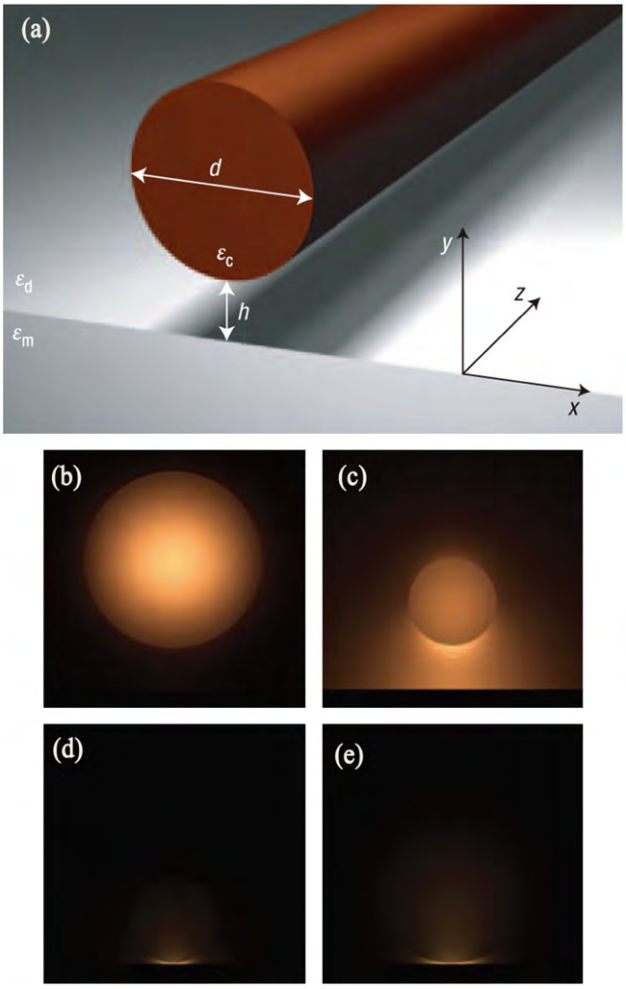

Figure 9 (a) The sketch of a hybrid optical waveguide. A dielectric cylindrical GaAs nanowire separated from a metal silver half-space by a nanoscale dielectric gap of SiO_2; (b)–(e) EM energy density distributions for $[d,h]=[400,100]$ nm, $[d,h]=[200,100]$ nm, $[d,h]=[200,2]$ nm, $[d,h]=[400,2]$ nm [111].

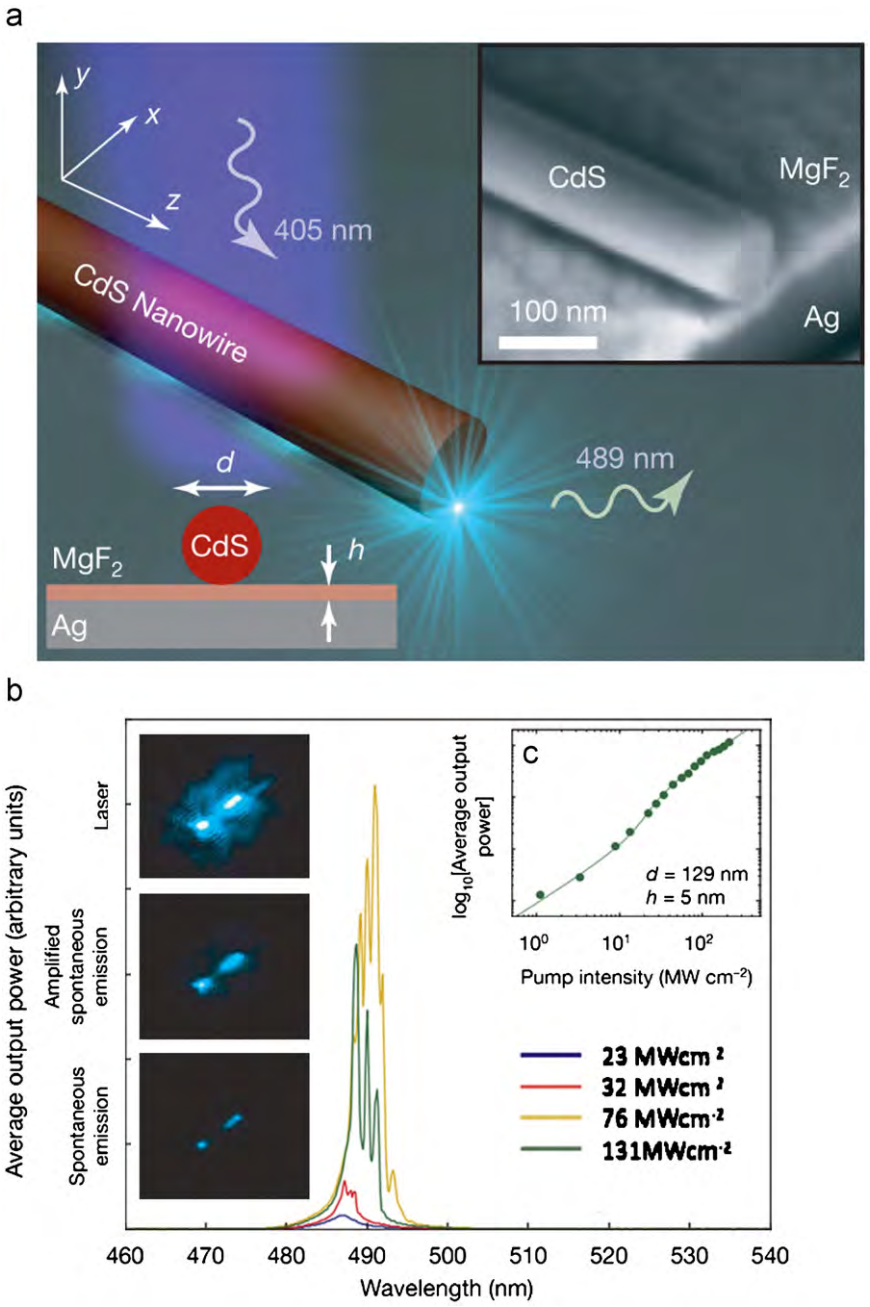

Figure 10 (a) The sketch of hybrid plasmonic laser which consists of a CdS semiconductor nanowire on top of a silver substrate separated by a nanometer-scale MgF_2 layer; (b) laser oscillation of a plasmonic laser at different pump intensity. The four spectra for different peak pump intensities exemplify the transition from spontaneous emission (21.25 MW cm^{-2}) via amplified spontaneous emission (32.50 MW cm^{-2}) to full laser oscillation (76.25 MW cm^{-2} and 131.25 MW cm^{-2}); (c) the nonlinear response of the output power to the peak pump intensity [20].

Dark mode and radiation of plasmonic lasing

SPs circumvent the diffraction limit and concentrate EM energy into areas substantially smaller than the wavelength. These plasmon modes can also be generated nonradiatively by the dark modes [113]. There have been extensive theoretical and experimental studies on the mechanism of excitation and propagation of dark modes. These modes exist in sub-diffraction-limited nanostructures without radiative losses and play an important role in integrated plasmonic nanophotonic devices [114–120]. Generally, both localized and delocalized SPs can be simultaneously generated. Their topologies are determined by separate small-scale ''hot spots'' that are distributed coherently over a distance comparable to the total size of the system [113]. By controlling the incident light from free space coupled to the plasmon modes, orders-of-magnitude differences in the coherence lengths and oscillator strengths are observed

from one mode to another at nearby frequencies. This creates the radiative mode and dark mode. Because of radiation coupled to the external forces, the radiative mode has a large scattering cross section and small Q factor. In comparison, the dark mode avoids radiation and interference from the outside. Therefore, dark modes always lead to a relatively large factor. Selection of dark eigenmodes for plasmonic lasing has been theoretically shown [7]. The size of the gain medium can be moderated to tune the transition frequency. At a given frequency, an eigenmode is selected by positioning the gain dots in the region where it local fields are maximum. The degree of localization of the dark or luminous eigenmodes in different energy transitions has also been illustrated.

Dark plasmon modes cannot be excited or observed from the far-field zone. They only exist in well confined near-field without coupling to the far zone optical field. Therefore, in the cavity of a plasmonic laser, the dark modes propagate along the metal-dielectrics interfaces without radiative loss and so the stimulated emission of SPs is amplified. The increased SP population benefits from the dark modes without radiation. It resembles an optical cavity with two reflectors with a reflectance at 100% allowing light to bounce back and forth when it passes through the gain medium. Consequently, a high Q factor and low threshold can be achieved.

Since the intense and highly trapped dark modes of SPs are confined to the local fields, there has been much interest in the associated light emission and lasing. Zheludev et al. used a metamaterial split-ring resonator to obtain light emission with high spatial coherence [18,121] (see Fig. 11). The weakly asymmetrical split-ring arrays show less radiation loss. In other plasmonic lasing devices, the response depends weakly on the mutual interactions between the individual elements in the structure, but in this high-Q resonator, the asymmetrical resonant ring arrays, in lieu of a single plasmonic resonator, break the overall symmetry of the local field. This leads to the luminous laser action fueled by trapped-mode plasmons. Meanwhile, if the asymmetry of the resonant split-ring is weak, strong plasma oscillations may exhibit small radiation losses associated with the electric and magnetic dipole emission of the antisymmetrical oscillating currents. Hence, the decay time can be lengthened. Although the asymmetry in the split ring may cause the coupling of radiative modes to free space, the situation can be improved by smaller asymmetry design for a larger Q-factor. Besides, using the optimized ring size, tunable amplification and lasing frequency of the plasmon modes can be achieved to match the luminescence resonance. Meanwhile, a large variety of gain media can be integrated due to the desirable feature offered by the thin-layer metamaterials split-ring resonator geometry.

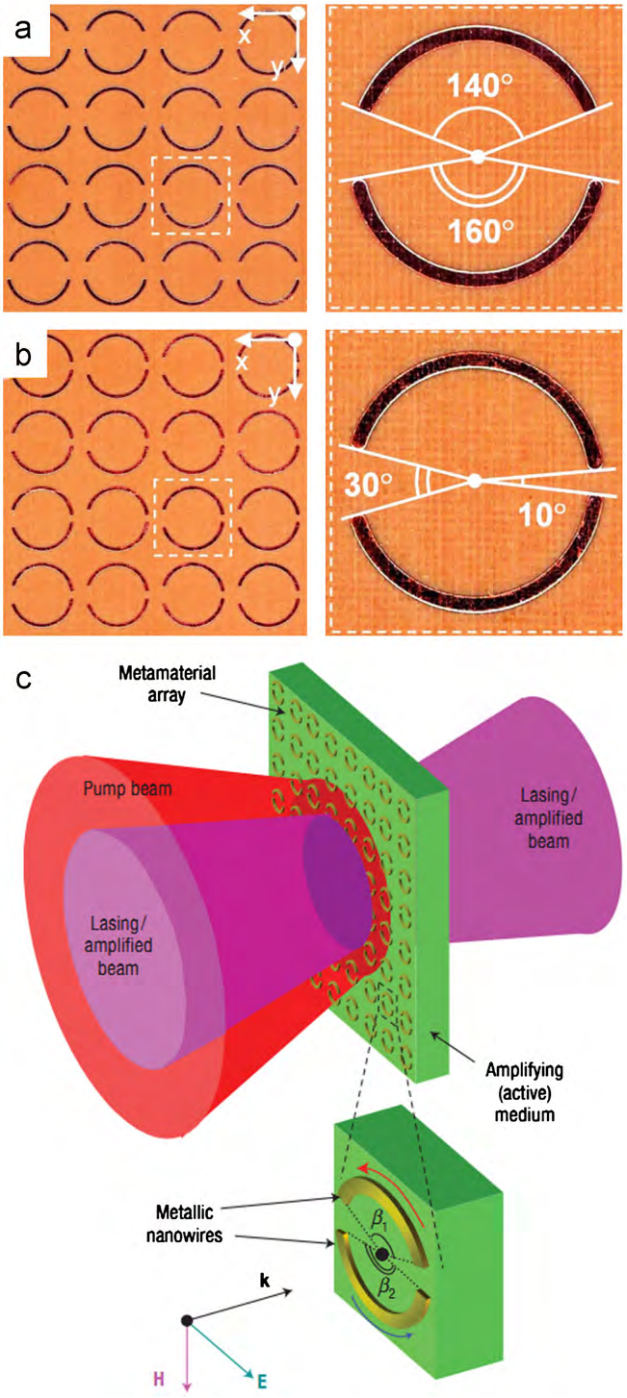

Figure 11 (a) and (b) Planar metamaterials with asymmetrically split copper rings [121]; (c) schematic of the lasing spaser structure by a metamaterial split-ring resonator with an array of weak asymmetry [18].

Outlook

In order to keep up the trend according to Moore's law, the microelectronics industry requires miniaturization and large-scale integration to achieve advanced performances while continuing to reduce cost. However, as integrated circuits enter the nano-regime, quantum effects enter into the design picture. Meanwhile, photonic devices must also provide ultra-fast transmission rate as well as high information capacity. Among the various obstacles, the diffraction limitation is one of the most serious issues plaguing miniaturization of photonic systems. Only if the diffraction limitation is overcome and light sources on the subwavelength scale are produced can the objective of fabricating tiny and ultra-fast photonic systems be fulfilled.

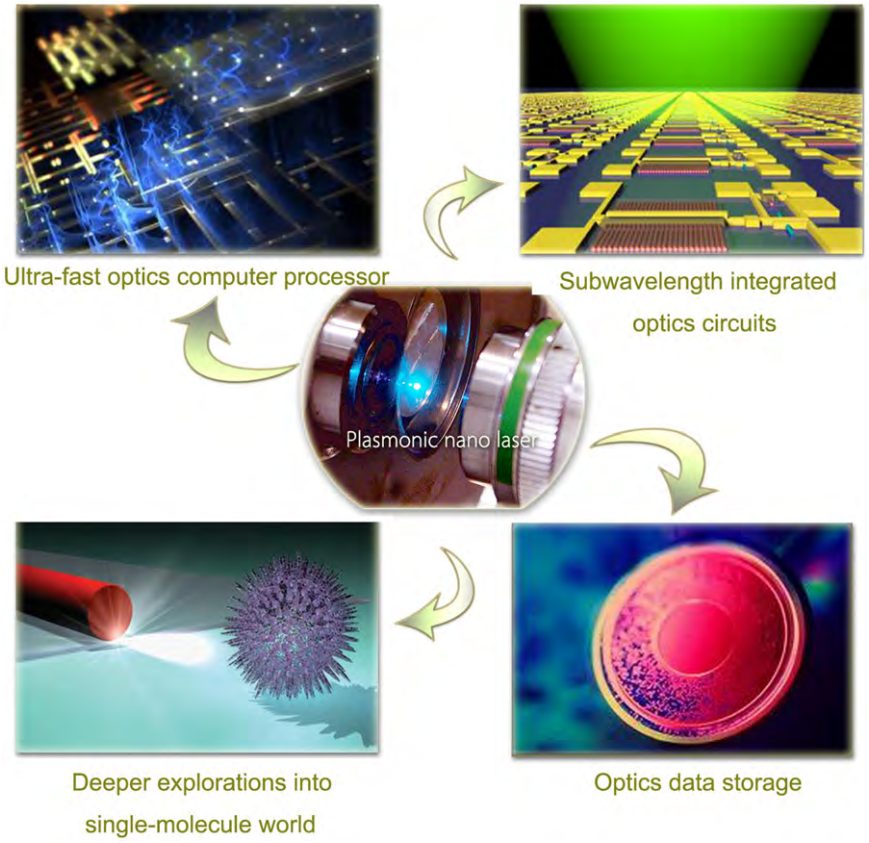

Figure 12 Potential applications provided by plasmonic nano-laser.

SPs bring the "light". Since SPs arise from surface collective electron oscillations on the metal-dielectric interface, the optical field fueled by SPs can be concentrated in nanoscale structures to circumvent the diffraction limitation. By adopting the plasmon modes with promising information carriers, plasmonic lasers boasting strong localized enhancement and subwavelength confinement can deliver high spatial localization well below the diffraction limit. Intense, coherent light beams are expected to pave the progress in nanoscale integrated photonic devices such as photonic chips. In addition, high-capacity EM data storage is possible with the aid of the high response speed and tiny light beam spot in plasmonic nano-laser systems. The extremely small, ultrafast, and coherent laser sources concentrate optical energy into subwavelength regions and provide the necessary tools to probe interesting science on the single molecular scale and explore new applications such as ultra-high-resolution biomedical diagnostics [122] (Fig. 12).

In spite of the tremendous potential, there are many challenges for nanoscale plasmonic laser integration. SPPs propagate along the metal surface freely together with other optical modes. This makes it difficult to achieve directional emission and produce the cavity feedback necessary for lasing. There are also problems associated with the optical pumping mechanism because different light signals can disrupt the propagation of the plasmon modes. The pumping energy delivered by optical sources tends to render the gain medium inefficient and localized heating further decreases the efficiency of gain compensation and lasing. In this respect, electrical pumping is an option. The desirable gain media should thus be adapted to electrical pumping and readily integratable into the laser system, not only to preclude interferences from unexpected optical modes but also to reduce localized heating of the tiny areas. Modulation of the laser frequencies and response speed is still required and can be accomplished by carefully designing the gain materials together with the geometry and size of the metal cavity.

Although many more challenges must be overcome before plasmonic nano-laser devices can become a stable energy source in the optoelectronics and electronics industry, big strides have recently been made. There is no doubt that intense light beams on the nanoscale are very useful and further study will enable better understanding of the nanoscale plasmonic world.

Acknowledgments

This work was jointly supported by the National Natural Science Foundation of China under grant nos. 51071045 and 11004026, Excellent Young Teachers Program of Southeast University, Hong Kong Research Grants Council (RGC) General Research Funds (GRF) No. CityU 112510, and City University of Hong Kong Research grant no. 9360110.

References

[1] A.L. Schawlow, C.H. Townes, Phys. Rev. 112 (1958) 1940–1949.
[2] M. Fujihira, H. Monobe, N. Yamamoto, H. Muramatsu, N. Chiba, K. Nakajima, T. Ataka, Ultramicroscopy 61 (1995) 271–277.
[3] L. Novotny, E.J. Sanchez, X.S. Xie, Ultramicroscopy 71 (1998) 21–29.
[4] P.F. Barbara, D.M. Adams, D.B. O'Connor, Annu. Rev. Mater. Sci. 29 (1999) 433–469.
[5] E.J. Sanchez, L. Novotny, X.S. Xie, Phys. Rev. Lett. 82 (1999) 4014–4017.
[6] H.G. Park, S.H. Kim, S.H. Kwon, Y.G. Ju, J.K. Yang, J.H. Baek, S.B. Kim, Y.H. Lee, Science 305 (2004) 1444–1447.
[7] D.J. Bergman, M.I. Stockman, Phys. Rev. Lett. 90 (2003) 027402.
[8] H. Raether, Surface Plasmons on Smooth and Rough Surfaces and on Gratings, Springer, Berlin, 1988.
[9] E. Ozbay, Science 311 (2006) 189–193.
[10] J.A. Conway, S. Sahni, T. Szkopek, Opt. Express 15 (2007) 4474–4484.
[11] M.L. Brongersma, V.M. Shalaev, Science 328 (2010) 440–441.
[12] A.V. Krasavin, A.V. Zayats, Opt. Express 18 (2010) 11791–11799.
[13] M.I. Stockman, Phys. Rev. Lett. 93 (2004) 137404.
[14] M.I. Stockman, J. Opt. 12 (2010) 024004.
[15] J.A. Gordon, R.W. Ziolkowski, Opt. Express 15 (2007) 2622–2653.
[16] M.A. Noginov, G. Zhu, A.M. Belgrave, R. Bakker, V.M. Shalaev, E.E. Narimanov, S. Stout, E. Herz, T. Suteewong, U. Wiesner, Nat. Mater. 460 (2009) 1110–1113.
[17] M.I. Stockman, Nat. Photonics 2 (2008) 327–329.
[18] N.I. Zheludev, S.L. Prosvirnin, N. PapasimakiS, V.A. Fedotov, Nat. Photonics 2 (2008) 351–354.
[19] E.M. Purcell, Phys. Rev. 69 (1946) 681.
[20] R.F. Oulton, V.J. Sorger, T. Zentgraf, R.M. Ma, C. Gladden, L. Dai, G. Bartal, X. Zhang, Nature 461 (2009) 629–632.
[21] K. Nozaki, S. Kita, T. Baba, Opt. Express 15 (2007) 7506–7514.
[22] A. Hatice, E. Dirk, V. Jelena, Nat. Phys. 2 (2006) 484–488.
[23] H. Ditlbacher, A. Hohenau, D. Wagner, U. Kreibig, M. Rogers, F. Hofer, F.R. Aussenegg, J.R. Krenn, Phys. Rev. Lett. 95 (2005) 257403.
[24] J. Schoenwald, E. Burstein, J.M. Elson, Solid State Commun. 12 (1973) 185–189.
[25] B. Lamprecht, J.R. Krenn, G. Schider, H. Ditlbacher, M. Salerno, N. Felidj, A. Leitner, F.R. Aussenegg, J.C. Weeber, Appl. Phys. Lett. 79 (2001) 51–53.
[26] J.C. Weeber, J.R. Krenn, A. Dereux, B. Lamprecht, Y. Lacroute, J.P. Goudonnet, Phys. Rev. B 64 (2001) 045411.
[27] T. Okamoto, F. H'Dhili, S. Kawata, Appl. Phys. Lett. 85 (2004) 3968–3970.
[28] C. Marquart, S.I. Bozhevolnyi, K. Leosson, Opt. Express 13 (2005) 3303–3309.
[29] T. Okamoto, J. Simonen, S. Kawata, Phys. Rev. B 77 (2008) 115425.
[30] T. Okamoto, J. Simonen, S. Kawata, Opt. Express 17 (2009) 8294–8301.
[31] I.R. Hooper, J.R. Sambles, Phys. Rev. B 65 (2002) 165432.
[32] I.R. Hooper, J.R. Sambles, Phys. Rev. B 66 (2002) 205408.
[33] D. Gerard, L. Salomon, F. de Fornel, Phys. Rev. B 69 (2004) 113405.
[34] I.R. Hooper, J.R. Sambles, Phys. Rev. B 70 (2004) 045421.
[35] B. Wang, L. Aigouy, E. Bourhis, J. Gierak, J.P. Hugonin, P. Lalanne, Appl. Phys. Lett. 94 (2009) 011114.
[36] K. Sakoda, Opt. Express 4 (1999) 167–176.
[37] U. Kreibig, M. Vollmer, Optical Properties of Metal Clusters, Springer, Heidelberg, 1995.
[38] M.D. Malinsky, K. Lance Kelly, G.C. Schatz, R.P. Van Duyne, J. Am. Chem. Soc. 123 (2001) 1471–1482.
[39] T. Qiu, X.L. Wu, Y.C. Cheng, G.G. Siu, P.K. Chu, Appl. Phys. Lett. 88 (2006) 143111.
[40] T. Qiu, X.L. Wu, J.C. Shen, P.K. Chu, Appl. Phys. Lett. 89 (2006) 131914.
[41] M. Quinten, A. Leitner, J.R. Krenn, F.R. Aussenegg, Opt. Lett. 23 (1998) 1331–1333.
[42] M.L. Brongersma, J.W. Hartman, H.A. Atwater, Phys. Rev. B 62 (2000) 16356–16359.
[43] K.H. Su, Q.H. Wei, X. Zhang, Nano Lett. 3 (2003) 1087–1090.
[44] Q.H. Wei, K.H. Su, S. Durant, X. Zhang, Nano Lett. 4 (2004) 1067–1071.
[45] W.H. Weber, G.W. Ford, Phys. Lett. B 70 (2004) 125429.
[46] D.S. Citrin, Nano Lett. 4 (2004) 1561–1565.
[47] S.G. Zou, G.C. Schatz, Phys. Rev. B 74 (2006) 125111.
[48] A.O. Pinchuk, G.C. Schatz, Mater. Sci. Eng., B 149 (2007) 251–258.
[49] V.A. Markel, A.K. Sarychev, Phys. Rev. B 75 (2007) 085426.
[50] S.A. Maier, P.G. Kik, H.A. Atwater, Appl. Phys. Lett. 81 (2002) 1714–1716.
[51] S.A. Maier, P.G. Kik, H.A. Atwater, S. Meltzer, E. Harel, B.E. Koel, A.A.G. Requicha, Nat. Mater. 2 (2003) 229–232.
[52] J.R. Krenn, J.C. Weeber, A. Dereux, E. Bourillot, J.P. Goudonnet, Phys. Rev. B 60 (1999) 5029–5033.
[53] A.M. Funston, C. Novo, T.J. Davis, P. Mulvaney, Nano Lett. 9 (2009) 1651–1658.
[54] J.C. Weeber, A. Dereux, Phys. Rev. B 60 (1999) 9061–9068.
[55] R.M. Dickson, L.A. Lyon, J. Phys. Chem. B 104 (2000) 6095–6098.
[56] N.M. Lawandy, Appl. Phys. Lett. 85 (2004) 5040–5042.
[57] N.M. Lawandy, Appl. Phys. Lett. 95 (2009) 234101.
[58] M.A. Noginov, G. Zhu, M. Bahoura, J. Adegoke, C.E. Small, B.A. Ritzo, V.P. Drachev, V.M. Shalaev, Opt. Lett. 31 (2006) 3022–3024.
[59] M.A. Noginov, G. Zhu, M. Bahoura, J. Adegoke, C. Small, B.A. Ritzo, V.P. Drachev, V.M. Shalaev, Appl. Phys. B 86 (2007) 455–460.
[60] R.R. Chance, A. Prock, R. Silbey, Adv. Chem. Phys. 37 (1978) 1–65.
[61] W.H. Weber, C.F. Eagen, Opt. Lett. 4 (1979) 236–238.
[62] J. Gersten, A. Nitzan, J. Chem. Phys. 75 (1981) 1139–1152.
[63] T. Qiu, F. Kong, X.Q. Yu, W.J. Zhang, X.Z. Lang, P.K. Chu, Appl. Phys. Lett. 95 (2009) 213104.
[64] A. De Luca, M.P. Grzelczak, I. Pastoriza-Santos, L.M. Liz-Marzan, M. La Deda, M. Striccoli, G. Strangi, ACS Nano 5 (2011) 5823–5829.
[65] M. Conforti, M. Guasoni, J. Opt. Soc. Am. B 27 (2010) 1576–1582.
[66] A. Alù, N. Engheta, Phys. Rev. B 74 (2006) 205436.
[67] A.F. Koenderink, A. Polman, Phys. Rev. B 74 (2006) 033402.
[68] C.R. Simovski, A.J. Viitanen, S.A. Tretyakov, Phys. Rev. E 72 (2005) 066606.
[69] R.A. Shore, A.D. Yaghjian, Electron. Lett. 41 (2005) 578–580.
[70] S.A. Maier, P.G. Kik, H.A. Atwater, Phys. Rev. B 67 (2003) 205402.
[71] A.V. Maslov, C.Z. Ning, IEEE J. Quantum Electron. 40 (2004) 1389–1397.
[72] D.S. Citrin, Opt. Express 31 (2006) 98–100.
[73] I.B. Udagedara, I.D. Rukhlenko, M. Premaratne, Phys. Rev. B 83 (2011) 115451.
[74] A.V. Maslov, C.Z. Ning, Appl. Phys. Lett. 83 (2003) 1237–1239.
[75] A.V. Maslov, C.Z. Ning, Opt. Lett. 29 (2004) 572–574.
[76] D.B. Li, C.Z. Ning, Phys. Rev. B 80 (2009) 153304.
[77] D.B. Li, C.Z. Ning, Appl. Phys. Lett. 96 (2010) 181109.

[78] M.T. Hill, M. Marell, E.S.P. Leong, B. Smalbrugge, Y.C. Zhu, M.H. Sun, P.J. van Veldhoven, E.J. Geluk, F. Karouta, Y.S. Oei, R. Nötzel, C.Z. Ning, M.K. Smit, Opt. Express (2003) 11107–11112.
[79] M.T. Hill, Y.S. Oei, B. Smalbrugge, Y.C. Zhu, T. de Vries, P.J. van Veldhoven, F.W.M. van Otten, T.J. Eijkemans, J.P. Turkiewicz, H. de Waardt, E.J. Geluk, S.H. Kwon, Y.H. Lee, R. Nötzel, M.K. Smit, Nat. Photonics 1 (2007) 589–594.
[80] W.L. Barnes, A. Dereux, T.W. Ebbesen, Nature 424 (2003) 824–830.
[81] M.I. Stockman, Phys. Rev. Lett. 106 (2011) 156802.
[82] D.E. Chang, A.S. Sorensen, P.R. Hemmer, M.D. Lukin, Phys. Rev. Lett. 97 (2006) 053002.
[83] Y.Y. Gong, J. Vuckovic, Appl. Phys. Lett. 90 (2007) 033113.
[84] A. Archambault, F. Marquier, J.J. Greffet, Phys. Rev. B 82 (2010) 035411.
[85] V.I. Klimov, A.A. Mikhailovsky, S. Xu, A. Malko, J.A. Hollingsworth, C.A. Leatherdale, H.J. Eisler, M.G. Bawendi, Science 290 (2000) 314–317.
[86] P.M. Bolger, W. Dickson, A.V. Krasavin, L. Liebscher, S.G. Hickey, D.V. Skryabin, A.V. Zayats (Eds.), Opt. Lett., 35, 2010, pp. 1197–1199.
[87] M. Ambati, D.A. Genov, R.F. Oulton, X. Zhang, IEEE J. Sel. Top. Quantum Electron. 14 (2008) 1395–1403.
[88] J. Seidel, S. Grafstrom, L. Eng, Phys. Rev. Lett. 94 (2005) 177401.
[89] J.K. Kitur, V.A. Podolskiy, M.A. Noginov, Phys. Rev. Lett. 106 (2011) 183903.
[90] M.A. Noginov, G. Zhu, M. Bahoura, C.E. Small, C. Davison, J. Adegoke, Phys. Rev. B 74 (2006) 184203.
[91] Y.H. Chen, J.F. Li, M.L. Ren, B.L. Wang, J.X. Fu, S.Y. Liu, Z.Y. Li, Appl. Phys. Lett. 98 (2011) 261912.
[92] I. De Leon, P. Berini, Nat. Photonics 4 (2011) 382–387.
[93] D. Sarid, Phys. Rev. Lett. 47 (1981) 1927–1930.
[94] G.I. Stegeman, J.J. Burke, D.G. Hall, Appl. Phys. Lett. 41 (1982) 906–908.
[95] T. Inagaki, M. Motosuga, E.T. Arakawa, J.P. Goudonnet, Phys. Rev. B 32 (1985) 6238–6345.
[96] R.K. Hickernell, D. Sarid, J. Opt. Soc. Am. B 3 (1986) 1059–1069.
[97] S.D. Gupta, G.V. Varada, G.S. Agarwal, Phys. Rev. B 36 (1987) 6331–6635.
[98] G. Winter, S. Wedge, W.L. Barnes, New J. Phys. 8 (2006) 125.
[99] P. Berini, Phys. Rev. B 61 (2000) 10484–10503.
[100] P. Berini, J. Appl. Phys. 98 (2005) 043109.
[101] P. Berini, C. Robert, L. Nancy, IEEE J. Sel. Top. Quantum Electron. 14 (2008) 1479–1495.
[102] I. De Leon, P. Berini, Phys. Rev. B 78 (2008) 161401.
[103] I. De Leon, P. Berini, Opt. Express 17 (2009) 20191–20202.
[104] M.C. Gather, K. Meerholz, N. Danz, K. Leosso, Nat. Photonics 4 (2010) 457–461.
[105] K. Unterrainer, R. Colombelli, C. Gmach, F. Capasso, H.Y. Hwang, A.M. Sergent, D.L. Sivco, A.Y. Cho, Appl. Phys. Lett. 80 (2002) 3060–3062.
[106] B.S. Williams, S. Kumar, H. Callebaut, Q. Hu, J.L. Reno, Appl. Phys. Lett. 83 (2003) 2124–2126.
[107] J.A. Fan, M.A. Belkin, F. Capasso, S. Khanna, M. Lachab, A.G. Davies, E.H. Linfield, Opt. Express 14 (2006) 11672–11680.
[108] C. Manolatou, F. Rana, IEEE J. Quantum Electron. 44 (2008) 435–447.
[109] D.A. Genov, R.F. Oulton, G. Barta, X. Zhang, Phys. Rev. B 83 (2011) 245312.
[110] M.P. Nezhad, A. Simic, O. Bondarenko, B. Slutsky, A. Mizrahi, L. Feng, V. Lomakin, Y. Fainman, Nat. Photonics 4 (2010) 395–399.
[111] R.F. Oulton, V.J. Sorger, D.A. Genov, D.F.P. Pile, X. Zhang, Nat. Photonics 2 (2008) 496–500.
[112] V.J. Sorger, Z.L. Ye, R.F. Oulton, Y. Wang, G. Bartal, X.B. Yin, X. Zhang, Nature Commun. 2 (2011) 331.
[113] M.I. Stockman, S.V. Faleev, D.J. Bergman, Phys. Rev. Lett. 87 (2001) 167401.
[114] S. Zhang, D.A. Genov, Y. Wang, M. Liu, X. Zhang, Phys. Rev. Lett. 101 (2008) 047401.
[115] M.Z. Liu, T.W. Lee, S.K. Gray, P.G. Sionnest, M. Pelton, Phys. Rev. Lett. 102 (2009) 107401.
[116] A.L. Koh, K. Bao, I. Khan, W.E. Smith, G. Kothleitner, P. Nordlander, S.A. Maier, D.W. McComb, ACS Nano 3 (2009) 3015–3022.
[117] M.W. Chu, V. Myroshnychenko, C.H. Chen, J.P. Deng, C.Y. Mou, F.J. Garcia de Abajo, Nano Lett. 9 (2009) 399–404.
[118] V. Klimov, G.Y. Guo, J. Phys. Chem. C 114 (2010) 22398–22405.
[119] Z.G. Dong, H. Liu, M.X. Xu, T. Li, S.M. Wang, J.X. Cao, S.N. Zhu, X. Zhang, Opt. Express 18 (2010) 22413–22417.
[120] C.G Biris, N.C. Panoiu, Nanotechnology 22 (2011) 235502.
[121] V.A. Fedotov, M. Rose, S.L. Prosvirnin, N. Papasimakis, N.I. Zheludev, Phys. Rev. Lett. 99 (2007) 147401.
[122] V.J. Sorger, X. Zhang, Science 333 (2011) 709–710.

Yin Yin received his BS degree in physics from Southeast University, China in 2009. He is currently a PhD candidate in the Department of Physics, Southeast University. His main research interests are metamaterials and plasmonics as well as their applications to nano-laser and optofluidic systems.

Teng Qiu received his BS in chemistry from Nanjing University, China in 2002 and PhD in condensed matter physics from Nanjing University in 2007. From 2004 to 2008, he was affiliated with Prof. Paul K. Chu's research group in City University of Hong Kong. He is currently a full professor of physics at Southeast University, China. In 2010, he was an Alexander von Humboldt fellow in the Leibniz Institute for Solid State and Materials Research in Dresden, Germany. His current research focuses on surface-enhanced spectroscopy. He has authored and co-authored about 60 refereed journal publications.

Jiaqi Li received his PhD degree in 2008 from Nanjing University. In 2009–2010, he worked as a research fellow in Nanyang Technological University, Singapore. He is currently a lecturer in the Physics Department of Southeast University and his research interests are nano-photonics and plasmonics.

Paul K. Chu received his BS in mathematics from The Ohio State University in 1977 and MS and PhD in chemistry from Cornell University in 1979 and 1982, respectively. He is the Chair Professor of Materials Engineering in the Department of Physics & Materials Science in City University of Hong Kong and holds advisory or visiting professorships in 13 universities and research institutes in China. Paul's research activities are quite diverse encompassing plasma science and engineering, surface engineering, and various types of materials and nanotechnology. Paul is the

co-editor of seven books on plasma science, biomedical engineering, and nanotechnology. He has co-authored more than 20 book chapters as well as 900 journal papers. He has also given more than 100 invited lectures and talks. He has been granted 11 US patents, 7 Chinese patents, and 1 European patent and founded 3 companies. He is the chairman of the Plasma-Based Ion Implantation (PBII&D) International Committee and a member of the Ion Implantation Technology (IIT) International Committee and IEEE Nuclear and Plasma Science Society (NPSS) Fellow Evaluation Committee. He is Fellow of the American Physical Society (APS), American Vacuum Society (AVS), Institute of Electrical and Electronics Engineers (IEEE), and Hong Kong Institution of Engineers (HKIE). He is the senior editor of IEEE Transactions on Plasma Science, associate editor of Materials Science & Engineering Reports, and editorial board member of 7 journals, including Biomaterials. He has won a number of awards, including the 2007 IEEE NPSS Merit Award and Materials Research Society (Taiwan) JW Mayer Lectureship. He was the general chair of the 3rd IEEE International NanoElectronics Conference in Hong Kong in 2010.